

Behaviour of thick concrete members with unbonded transverse reinforcement

Mathieu Fiset¹, Alexandra Parenteau¹, Sébastien Bilodeau¹, Josée Bastien¹ and Denis Mitchell²

¹ *Research Center on Concrete Infrastructure (CRIB),
Université Laval,
1065 Avenue de la Médecine, Québec (G1V 0A6), Québec, Canada,*

² *Research Center on Concrete Infrastructure (CRIB),
McGill University,
817 Sherbrooke Street West, Montréal (H3A 0C3), Québec, Canada,*

Abstract

One commonly used method to increase the shear capacity of existing concrete structures consists of adding vertical steel bars anchored to the structure by means of mechanical anchorages, such as expansion torque controlled anchorages or steel anchorage plates. If the drilled holes are not filled with adhesive then the bars are unbonded along their length. In order to study the behaviour of concrete members with unbonded transverse reinforcement, thick concrete beams (width of 610 mm and height of 750 mm) were loaded until shear failure. It has been observed that their shear capacity is closely related to the shear cracking behaviour. At shear cracking, the propagation of one large diagonal crack is required to activate the vertical unbonded bars, thereby reducing the aggregate interlock shear capacity along the cracks. Beams containing at least minimum amounts of conventional stirrups experience several diagonal cracks at shear failure, whereas a beam with unbonded bars tends to have one dominant crack and can therefore experience the size effect in shear. A finite element (FE) model was also used to study the parameters influencing the behaviour of concrete members with unbonded transverse bars. The finite element results show very good agreement with the experimental results.

1 Introduction

Thick slabs are a commonly used structural form for small and medium span bridges. Existing thick concrete slabs have depths ranging from 600 mm to 2500 mm, spans ranging from 15 to 25 m and a deck width to match the width needed for the traffic lanes. For many of these older bridges, it was typically assumed that the depth of the concrete slab was able to fully resist the shear stresses and therefore shear reinforcement was not required. However, due to the size effect in shear and combined to the increase of traffic loads and material degradation, many of these thick slabs need to be strengthened in shear.

One commonly used method to increase the shear capacity of existing concrete beams consists of adding transverse shear reinforcement. Several researchers have studied the addition of GFRP, CFRP strips or bars anchored to the side faces of beams using epoxy adhesive or cement mortar (Barros, J. A. P. and Dias, S. J. E., 2006, Adhikary, B. B. and Mutsuyoshi, H., 2006, Al-Mohamoud, F. *et al.* 2009 and De Lorenzis, L. and Nanni, A., 2001). However, these methods are not effective for wide, thick concrete slabs. Transverse reinforcing bars have therefore to be distributed along the length and width of thick slabs, inserted and anchored into the existing structure. Vertical steel reinforcing bars introduced into vertical pre-drilled holes and bonded to the concrete with epoxy adhesive along the full bar length was previously investigated (Fernández-Ruiz, M. *et al.* 2010 Provencher, P., 2011). and proved to be an excellent technique for increasing the shear capacity.

Another way to anchor the added transverse bars to the concrete is to use mechanical anchorages, such as expansion torque controlled anchorages or bolted steel plates. However, because the bar is not bonded to the concrete, it is expected that this added reinforcement will not be as effective as conventional stirrups that are bonded to the concrete and anchored by hooks at their ends. To study the effectiveness of this type of transverse reinforcement, three experiments were carried out, finite element

(FE) models of the tested members were developed and the predictions were compared with the experimental results.

2 Experimental program

Experimental tests were performed on slab slices (beams) strengthened with unbonded transverse reinforcement. Specimen “T” contains transverse reinforcement anchored into the member with torque controlled expansion anchorages (Fig. 1a and b). When torqued, the shell of the mechanical anchorage expands and exerts lateral pressure on the internal surfaces of the hole, which produces a frictional force and anchors the reinforcing bar. Specimen “P” contains unbonded transverse reinforcement anchored to the top and the bottom member faces with bolted plates (Fig. 1c). The slab properties and strengthening details are summarized in Table 1 and Fig. 2 (Provencher, P., 2011). These slabs span 4 m, have a height of 750 mm and a width of 610 mm. Slab “S” contains conventional stirrups as required by North American standards (CSA S6-14 (Canadian Standards Association, 2014)) and is used to compare the responses of bonded and unbonded transverse reinforcement. Note that transverse bars spacing s_v in the members S and T is 380 mm ($s_v/d_v=0.61$), while it is 1000 mm for the specimen P ($s_v/d_v = 1.60$). The longitudinal reinforcement ratio is 1.65% and the flexural lever arm d is 694 mm. Specimens were loaded at mid-span and the shear span to depth ratio a/d is 2.88 (Fig. 3a). After failure occurred in one shear span this end of the beam was strengthened using external shear clamps and then the other shear span was loaded to failure. The yield strengths f_y of the transverse bars are shown in Table 1. For the longitudinal bars, f_y is 508 MPa and, for all bars, the steel Young’s modulus E_s is taken as 200 GPa. The maximum aggregate size (a_g) of the concrete is 19 mm and the concrete cylinder compressive strengths (f_c) obtained on the testing day are presented in Table 1. According to the manufacturer, the maximum tensile capacity of the torque controlled anchor is 93.6 kN for the strength of concrete used.

Table 1 Details of slab specimens

Name	Anchorage of transverse bars	s_v [mm]	d_v [mm]	s_v/d_v	d_{bv} [mm]	A_v [mm ²]	f_y [MPa]	f_u [MPa]	f_c [MPa]
T	Torque controlled	380	625	0.61	13.6	292	642	800	31.5
P	Two anchor plates	1000	625	1.60	28.7	1290	517	689	31.2
S	Stirrups	380	625	0.61	15.9	400	448	633	33.3

d_v : Effective shear depth, taken as $0.9d$;

d_{bv} : Transverse reinforcement bar diameter

A_v : Shear reinforcement area within a distance s_v ,

f_u : Shear reinforcement ultimate strength

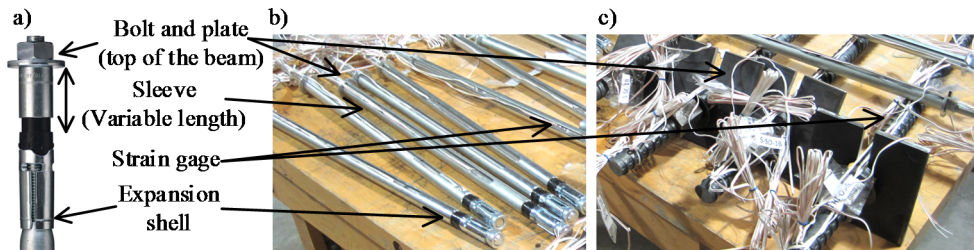


Fig.1 Details of anchor systems. a) Torque controlled expansion anchorage description and anchorage used for b) the specimen T. c) Bolted anchor plated used for the specimen P.

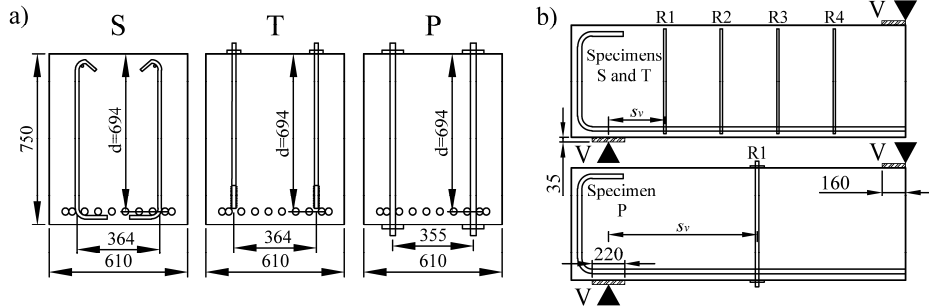


Fig. 2 a) Section details and b) profile view (half span) of tested specimens (dimensions in mm)

As shown in Fig. 1, strain gages were installed on the transverse reinforcing bars to measure axial strains. LVDTs in the form of rosettes were installed on the side faces of the beams (see Fig. 3b) at the quarter points of the span (1000 mm from the support) to measure the crack width and the crack slip. By knowing the crack angles θ , the horizontal and the vertical displacements u_x and u_y are given by the rosette and the crack width w and slip s can be estimated from Eq. (1).

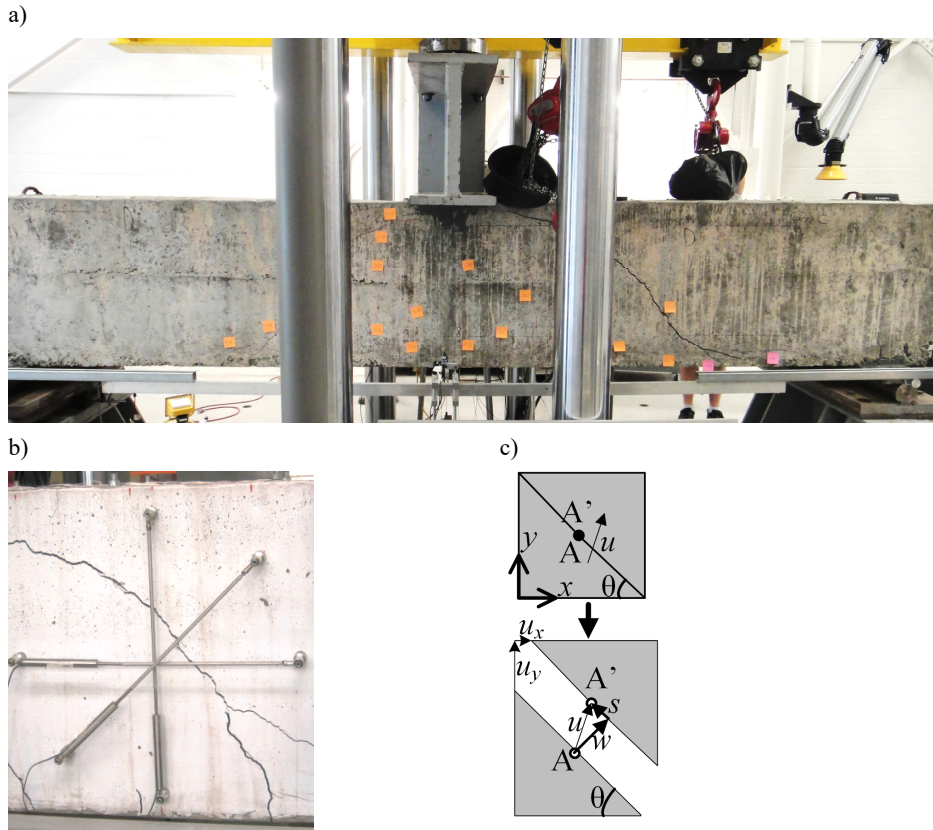


Fig.3 a) Testing setup, b) LVDTs rosette for crack width measurement, c) crack width and slip

$$\begin{Bmatrix} w \\ s \end{Bmatrix} = \begin{bmatrix} \sin \theta & \cos \theta \\ -\cos \theta & \sin \theta \end{bmatrix} \begin{Bmatrix} u_x \\ u_y \end{Bmatrix} \quad (1)$$

3 Numerical modelling

The predicted responses of the test specimens were obtained using VecTor2, a non-linear finite elements (FE) program for reinforced concrete structures. VecTor2 software uses two dimensional membrane finite elements with rotating smeared cracks model based on the Modified Compression Field theory (MCFT) (Vecchio, F. J. and Collins, M. P., 1986 and Wong P.-S., 2002) It offers several options in terms of materials behaviour and element library. The modelling of the concrete and steel stress-strain relationships are illustrated in Fig. 4. A trilinear stress-strain relationship is used for steel. The concrete stress-strain relationships were chosen according to the Attard & Setunge 1996 model in compression and the Yamamoto (2001) model in tension (Fig. 4c). The tension stiffening and compression softening effects are also included according to Bentz 2003 and Vecchio 1992 models. All equations and references can be found in the VecTor2 references (Wong P.-S., 2002).

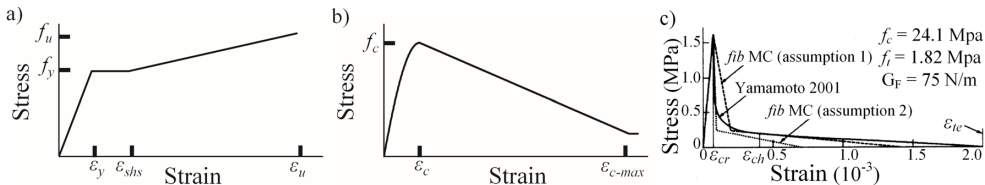


Fig.4 (a) Steel behaviour and concrete behaviour in b) compression and c) tension [10]

The meshes, boundary conditions and elements used for the predictions are shown in Fig. 5. Taking into account the symmetry of geometry and loading, half of the slab was modelled. For the boundary conditions, the horizontal displacements are restrained at mid-span and vertical displacements are restrained at the support. All specimens were modelled with 2D membrane elements. The steel plates at the support and at the loading location as well as the anchor plates of transverse bars were modelled using steel membrane elements and bearing elements. These bearing elements were introduced between steel and concrete elements to carry only unidirectional forces and avoid confinement. The shear reinforcement was modelled with discrete truss elements and longitudinal reinforcing bars with a smeared steel concrete approach. The truss elements used for the unbonded bars were only connected to the concrete at node representing the anchor plates or to a concrete element node for the torque controlled expansion anchorage (see Fig 5). Unlike the unbonded bars, the truss elements used for the stirrups in specimen S were perfectly linked to the concrete element nodes over their lengths.

4 Results and discussion

Experimental results as well as FE results are compared in Figures 5 and 6 as well as in Table 2. Fig. 5 illustrates the observed cracking pattern and the predicted cracking. The shear, V , versus the deflection responses of the specimens as well as the variation of crack width, w , slip, s , and bar strain are presented in Fig. 6. Note that because each member was loaded twice, the first loading is used to compare cracking and behaviour (Fig. 5 and 6) while the average of the two loadings is used to compare the maximum shear capacities (Table 2). Transverse bar strains are presented in Fig. 6b. The shear failure is illustrated by the marker "X" while the steel yielding strain ($\epsilon_y = f_y/E_s$) is identified by a dashed horizontal line. No experimental steel strain measurements are available for specimen T. This is due to the torquing of the transverse reinforcement anchorage that damaged the strain gage. Numbering of the transverse reinforcement is described in Fig. 2.

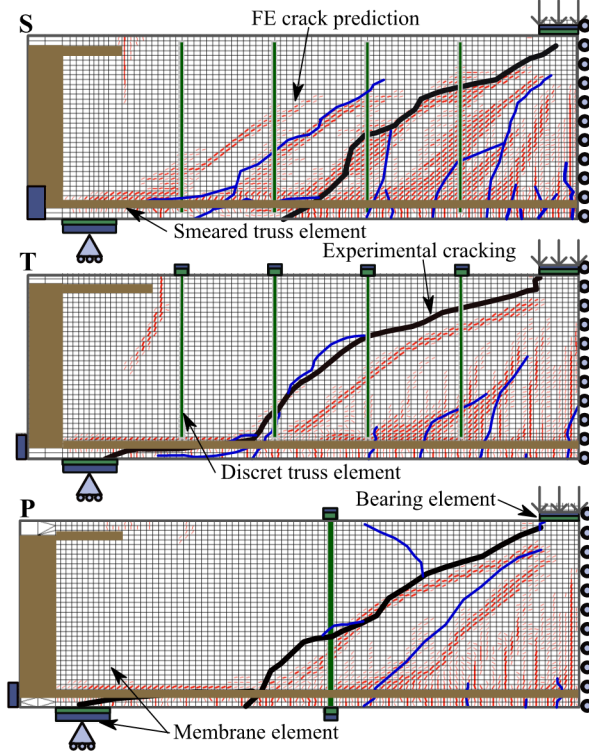


Fig 5. Experimental cracking pattern and comparison to FE predictions

4.1 Experimental observations

From the cracking pattern presented in Fig 5, it can be seen that the specimen with conventional stirrups exhibits a greater number of diagonal cracks than the members with unbonded bars. As shown by the cracking response in Fig. 6, the crack width increases slowly from the cracking load up to the failure of member S. Compared to specimen S, specimens T and P experienced a sudden increase in crack width and slip immediately after shear cracking. After shear cracking there was a decrease in the shear load and is associated with the rapid progression of a diagonal shear crack. After diagonal cracking, the tensile strain in the bars increases from 0.140 to 0.650 millistrain (28 to 130 MPa), and progresses up to 0.935 millistrain.

Before the failure of specimen P, a second shear crack appeared, illustrated with a thinner blue line in Fig. 5, between the transverse bar and the loading location. This crack was not measured by the rosette. This cracking caused a small reduction of the load and a reduction of the measured main shear crack width and slip as shown in Fig. 6a. The force in the transverse bars also decreased with the development of this crack. Thus, even if specimens with unbonded bars contain fewer diagonal cracks than the specimen with conventional stirrups, the unbonded shear reinforcement in specimen P allowed the formation of new diagonal cracks after reaching the first shear cracking.

As expected, the crack width at failure is smaller for the specimen with conventional stirrups than for the specimens with unbonded bars. For specimen S, $w = 2.52$ mm, while $w = 4.73$ mm and 3.59 mm for specimens T and P, respectively. It can therefore be expected that the concrete aggregate interlock resistance, which decreases with increasing crack width, is less for specimens T and P than for specimen S. At failure of all tested specimens, the crack slipped and the crack width increased. The bar strain increased but remained below the bar yield strength (517 MPa, or 2.59 millistrain) for specimen P.

4.2 Flexibility of the anchor plate

To take into account the flexibility of the transverse reinforcement anchor system in the FE model, the vertical displacement measured by the LVDTs and the elongation of the bar determined from the measured strain are compared. At failure of the specimen P, the vertical measured displacement is

4.20 mm while the bar elongation is 1.30 mm. It can be found that the equivalent bearing Young's modulus reproducing the flexibility of the anchor system is about 1600 MPa. For the specimen T, it is assumed that the stiffness of the anchor plate is similar to that for specimen P. For the torque controlled anchorage, Collins et al. (1989) have shown that the sleeve displacement is negligible before the failure of the anchorage. The flexibility of the torque controlled anchorage is therefore not considered in the model.

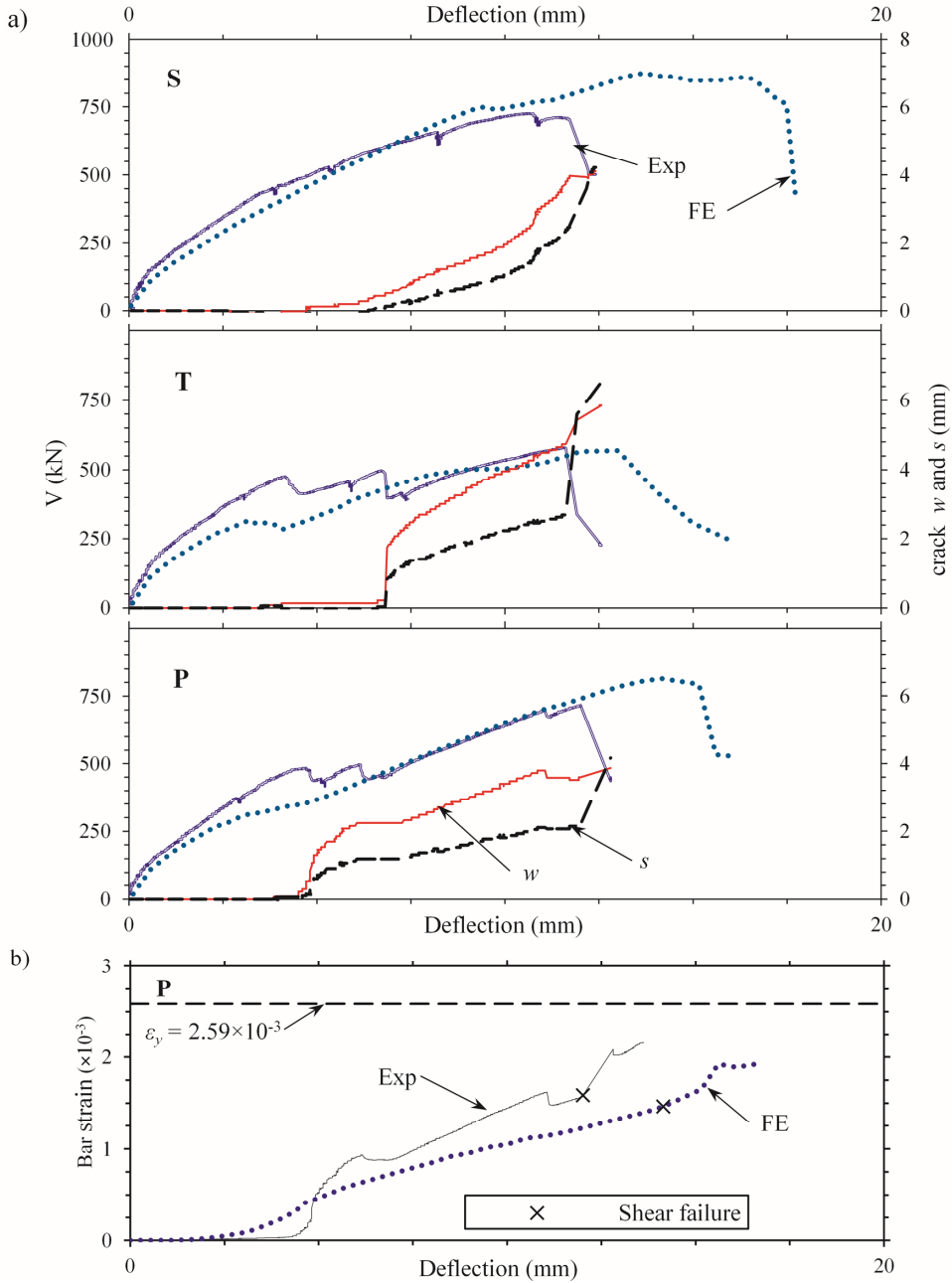


Fig. 6 Tested specimens response and FE predictions, a) load to deflection and cracking behaviour and b) axial strain gage of unbonded transverse reinforcement (R1)

4.3 Comparison to standard method and FE model

Table 2 shows the average maximum shear capacities and deflection at failure for the two half spans of each tested slab slices. For comparison purposes, shear capacities V_{CSA} predicted by the current Canadian Standards for bridge design (Canadian Standards Association, 2014 and Collins, M.P., 1996) are presented. Although the general method for shear strength of elements with stirrups is for convention bonded stirrups it was used to determine the maximum shear capacity of the specimens with unbonded bars. It can be seen that the capacity of the specimen with conventional stirrups is well predicted ($V_{CSA}/V_{exp} = 1.05$). However, as expected, the shear capacity of specimens T and P is largely overestimated due to the fact that the “stirrups” are unbonded with $V_{CSA}/V_{exp} = 1.39$ and 1.12, respectively. The design method for elements with conventional bonded shear reinforcement like stirrups is therefore not recommended for unbonded shear reinforcement. In such cases, FE models are more appropriate to predict the shear capacities.

Table 2 Summary of results (average of two experimental tests)

Slabs	V_{exp} [kN]	Δ_{exp} [mm]	V_{CSA} [kN]	V_{FE} [kN]	Δ_{FE} [mm]	V_{CSA}/V_{exp}	V_{FE}/V_{exp}	Δ_{FE}/Δ_{exp}
S	768	10.7	804	876	13.7	1.05	1.14	1.28
T	585	11.3	810	570	13.0	1.39	0.97	1.15
P	843	15.6	920	815	14.1	1.12	0.97	0.91
Average						1.18	1.03	1.11
Coefficient of variation (cov)						0.16	0.09	0.17

Comparisons between the experimental results and the predicted responses using the FE model are presented in Fig. 5, Fig. 6 and Table 2. Generally, it can be observed that the FE model with the appropriate anchor stiffness gives very good predictions of the behaviour of the specimens.

It can be seen in Fig. 6a that, before shear cracking, the predictions using the FE models give almost the same stiffness as the experimental curves. For specimen S, the experimental shear cracking load is similar to the predicted one by the finite elements model. For specimens with unbonded bars, the experimental shear cracking load is higher than the finite elements predictions, by about 160 kN. It is noted that there is variation between the shear strengths of one end of the beam versus the other end with two peaks associated with the experimental shear cracking (see Fig. 6a) while the FE analysis gives one predicted response curve. It can also be observed that the load decrease after the shear cracking of specimens T and P is greater for the experimental tests than for the finite elements model predictions. This is likely due to a more gradual increasing of the crack width at shear cracking in the FE model compared to that in the experimental test. This explanation is confirmed through the progression of the bar strain in Fig. 6b. The increase of bar strain for specimen P is more gradual than the experimental response, but the overall behaviour and the strain at failure are similar in both the finite elements prediction and the experimental results. This difference in the cracking behaviour may be due to the bond model between the longitudinal bars and the concrete in the FE analysis. For specimens T and P, a longitudinal splitting crack appeared rapidly after shear cracking. In the FE model, the smeared longitudinal bars are assumed perfectly linked to the concrete. With a higher bond, the number of cracks increased and the cracking load decreases (Oh, B.H *et al.*, 2007). In such a case, the shear cracking and the splitting crack appeared sooner, but their progression is reduced compared to the experimental cracking.

By using the FE model, very good predictions of the shear capacities were achieved. The ratio between the predicted and experimental shear capacities (V_{FE}/V_{exp}) presented in Table 2 is 1.03 in average (COV of 0.09). The deformation capacity (Δ_{FE}/Δ_{exp}) is overestimated by 11% in average (COV of 0.17) by the model, which is relatively good. The good agreement between the predicted cracking patterns and the observed ones in Fig. 5 confirm that the predictions using the FE model are reasonable. For specimens T and P, a similar number of cracks are observed but, the FE model predicts cracks closer to the loading location than the experimental pattern. For specimen S, the FE model predicts one additional diagonal crack near the support compared with the observed pattern. However, it can be seen that the experimental and predicted critical shear cracks leading to shear failure, illustrated in black and red bold line respectively, are closely located. The FE model and the experimental

results indicate that the critical shear crack intercepts the same number of transverse bars. This leads to a very good prediction of the member behaviour.

5 Conclusions and future work

This paper presents the behaviour of concrete thick slab slices strengthened in shear with drilled-in unbonded shear reinforcement. Shear reinforcing bars were only anchored to the concrete at their extremities by anchor plates or torque controlled expansion anchorage.

The experimental program demonstrated that specimens with unbonded transverse reinforcement contain less shear cracks than the companion specimen with conventional stirrups. The behaviour of members with unbonded bars is strongly influenced by the presence of a large diagonal crack. The analysis shows that the formation of the shear cracking is sudden for members with unbonded bars while it is more gradual when conventional stirrups are used. When unbonded bars are used, the shear crack width at failure is also larger than in a beam with conventional stirrups. A large crack is required to activate the unbonded transverse reinforcement in order to carry a higher shear. A lower aggregate interlock shear resistance occurs for members with unbonded bars than for conventional stirrups. At failure, the specimens with unbonded bars did not reach their yield strength and the specimens failed by concrete crushing. These two factors explain why standards used for member with stirrups are not applicable for elements with unbonded bars.

By taking into account the flexibility of the anchorages of the transverse reinforcement in the finite element analysis, it was possible to accurately predict the complete responses of the members with unbonded bars. The use of finite elements analysis enabled a better understanding of the behaviour of concrete members. In the future, it is expected that finite elements models will be used to analyse the complete behaviour of concrete members strengthened in shear with unbonded reinforcing bars.

References

- Adhikary, B.B.; Mutsuyoshi, H.: Shear strengthening of reinforced concrete beams using various techniques. In: *Construction and Building Materials* (2006) No. 20, pp. 366-373
- Al-Mahmoud, F., Castel, A., François, R., Tourmeur, C.: Strengthening of RC members with near-surface mounted CFRP rods. In: *Composite Structures* (2009). No. 91, pp. 138-147
- Barros, J.A.O.; Dias, S.J.E.: Near surface mounted CFRP laminates for shear strengthening of concrete beams. In: *Cement & Concrete Composites* (2006) No. 28, pp. 276-292
- Canadian Standards Association: *Canadian Highway Bridge Design Code* (2014)
- Collins, D.M., Klinger, R.E., Polyzois, D.: Load-deflection behavior of cast-in-place and retrofit concrete anchors subjected to static, fatigue and impact tensile loads. Center for transportation research, University of Texas at Austin (1989). Report 1126-1, 217 pages
- Collins, M.P., Mitchell, D., Adebar, P. and Vecchio, F.J.: A general shear design method. In: *ACI Structural Journal* (1996). V. 93, pp. 36-45.
- De Lorenzis, L., Nanni, A.: Shear Strengthening of Reinforced Concrete Beams with Near-Surface Mounted Fiber-Reinforced Polymer Rods. In: *ACI Structural Journal* (2001). No. 1 pp. 60-68
- Fernández-Ruiz, M., Muttoni, A., Kunz, J.: Strengthening of Flat Slabs Against Punching Shear Using Post-Installed Shear Reinforcement. In: *ACI Structural Journal* (2010). No. 4, pp. 434-442.
- Oh, B.H., Kim, A.H.: Advanced Crack Width Analysis of Reinforced Concrete Beams under Repeated Loads (2007). In: *ASCE Journal of structural engineering*. V. 133, pp. 411-420.
- Provencher, P.: Renforcement des dalles épaisses en cisaillement (master thesis). In: *Département de génie civil, Université Laval, Québec, Canada* (2011)
- Vecchio, F.J.; Collins, M.P.: The Modified Compression Field Theory for Reinforced Concrete Elements Subjected to Shear. In: *ACI Journal* (1986) No.2, pp. 219-231
- Wong, P.-S., Vecchio, F.J.: *VecTor2 and FormWorks User's Manual* (2002), 213p.
- Yamamoto, T., Vecchio, F.J.: Analysis of Reinforced Concrete Shells for Transverse Shear and Torsion. In: *ACI Structural Journal* (2001). V.127, pp.350-358